International Journal of Nanomedicine

Dovepress
open access to scientific and medical research

Open Access Full Text Article

ORIGINAL RESEARCH

Greater Plasma Protein Adsorption on Mesoporous Silica Nanoparticles Aggravates Atopic Dermatitis

Jin Kyeong Choi[1,*], Jun-Young Park[2,*], Soyoung Lee[3], Young-Ae Choi[4], Song Kwon[2], Min Jun Shin[2,5], Hui-Suk Yun[6], Yong Hyun Jang[7], Jinjoo Kang[4], Namkyung Kim[4], Dongwoo Khang[2,5,8], Sang-Hyun Kim[4]

[1]Department of Immunology, Jeonbuk National University Medical School, Jeonju, 54907, Republic of Korea; [2]Lee Gil Ya Cancer and Diabetes Institute, Gachon University, Incheon, 21999, Republic of Korea; [3]Immunoregulatory Materials Research Center, Korea Research Institute of Bioscience and Biotechnology, Jeongeup, 56212, Republic of Korea; [4]CMRI, Department of Pharmacology, School of Medicine, Kyungpook National University, Daegu, 41944, Republic of Korea; [5]Department of Health Sciences and Technology, GAIHST, Gachon University, Incheon, 21999, Republic of Korea; [6]Powder & Ceramics Division, Korea Institute of Materials Science, Changwon, 51508, Republic of Korea; [7]Department of Dermatology, School of Medicine, Kyungpook National University, Daegu, 41944, Republic of Korea; [8]Department of Physiology, School of Medicine, Gachon University, Incheon, 21999, Republic of Korea

*These authors contributed equally to this work

Correspondence: Dongwoo Khang, Department of Physiology, School of Medicine, Gachon University, Incheon, 21999, Republic of Korea, Tel +82 32 899 6515, Email dkhang@gachon.ac.kr; Sang-Hyun Kim, Department of Pharmacology, School of Medicine, Kyungpook National University, Daegu, 41944, Republic of Korea, Tel +82 53 420 4838, Email shkim72@knu.ac.kr

Purpose: The protein corona surrounding nanoparticles has attracted considerable attention as it induces subsequent inflammatory responses. Although mesoporous silica nanoparticles (MSN) are commonly used in medicines, cosmetics, and packaging, the inflammatory effects of the MSN protein corona on the cutaneous system have not been investigated till date.

Methods: We examined the greater plasma protein adsorption on MSN leads to serious inflammatory reactions in *Dermatophagoides farinae* extract (DFE)-induced mouse atopic dermatitis (AD)-like skin inflammation because of increased uptake by keratinocytes.

Results: We compare the AD lesions induced by MSN and colloidal (non-porous) silica nanoparticles (CSN), which exhibit different pore architectures but similar dimensions and surface chemistry. MSN-corona treatment of severe skin inflammation in a DFE-induced in vivo AD model greatly increases mouse ear epidermal thickness and infiltration of immune cells compared with the CSN-corona treatment. Moreover, MSN-corona significantly increase AD-specific immunoglobulins, serum histamine, and Th1/Th2/Th17 cytokines in the ear and lymph nodes. MSN-corona induce more severe cutaneous inflammation than CSN by significantly decreasing claudin-1 expression.

Conclusion: This study demonstrates the novel impact of the MSN protein corona in inducing inflammatory responses through claudin-1 downregulation and suggests useful clinical guidelines for MSN application in cosmetics and drug delivery systems.

Keywords: protein Corona, atopic dermatitis, mesoporous silica, colloidal silica, claudin-1, immunotoxicity

Introduction

Nanomaterials have been increasingly applied in various fields such as biology, chemistry, physics, medicine, and engineering.[1–3] Colorless amorphous silica nanoparticles and titanium dioxide (TiO_2), which reflect ultraviolet light more effectively than fine particles, are widely used as practical components in various cosmetics such as sunscreens and foundation creams.[4] Specifically, silica nanoparticles exhibit high transparency and coatability, which enable their use as anti-caking agents in food or as base material in cosmetics.[5] Increasing applications of nanomaterials in healthcare-related industries will presumably lead to unforeseeable toxicity.[6,7] Nanoparticles can enter the body via different routes, such as the gastrointestinal tract, lungs, and skin.[8] The skin is a major route for exposure to external materials because of its easy accessibility and large surface area.[9] In addition, nanoparticles can interact with many plasma proteins; the phenomenon of non-specific binding between plasma proteins and nanoparticles is called a protein-corona.[10,11] The newly formed protein corona around the nanoparticles can affect the activation of the immune system.[12–14] Previous studies have clearly shown that altering the protein structure of nanoparticles can affect the immune-active function of

Received: 22 July 2022
Accepted: 22 September 2022
Published: 29 September 2022

Graphical Abstract

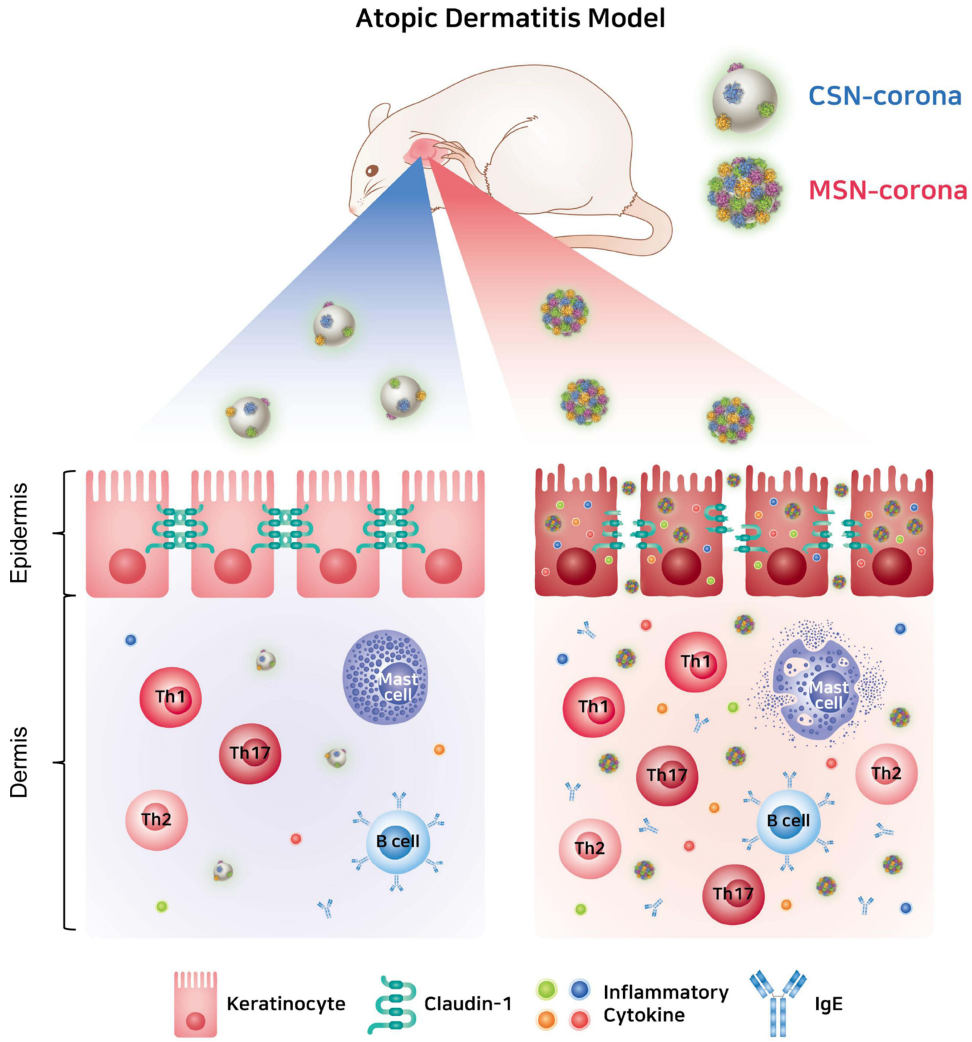

immune cells.[14,15] In particular, immunostimulatory proteins are highly sensitive to their interactions with nanoparticles, because of which the immune system directly reacts to the unfolded plasma structure.[14,15] Previous studies have revealed that immune-inducing proteins react with nanoparticles to induce considerable structural changes and that more marked changes in protein structure induce subsequent inflammatory responses both in vitro and in vivo.[14,15]

Atopic dermatitis (AD) is a chronic allergic inflammatory skin disease characterized by dryness, eczema, pruritus, and skin hyperreactivity to environmental triggers.[16] House dust mites (HDMs) such as *Dermatophagoides farinae* are among the most important environmental allergens related to human AD. HDM allergens contribute to AD pathogenesis by inducing both acute and chronic AD lesions.[17] Acute AD lesions are characterized by elevated serum IgE levels, epidermal and dermal thickening, dermal infiltration of eosinophils, and Th2 and Th17 cytokines. Chronic AD skin lesions are characterized by epidermal hyperplasia that is mediated by Th1 and Th22 cytokines, increased collagen deposition in the dermis, and dry fibrotic papules.[18] Additionally, tight junctions are key contributors to the epidermal barrier, and claudin-1, an important component in epidermal tight junctions, is crucial for skin barrier function.[19] Claudin-1 was shown to be reduced in the skin lesions of patients with AD, triggering skin inflammation.[20] For patients with AD, severe eczema or excessive exposure to sunlight may worsen their symptoms. Using sunscreen to protect the skin from sunlight can alleviate skin barrier dysfunction

and reduce inflammation and facial redness.[21] However, sunscreen commonly can cause side effects in patients with AD. The recommendation to use sunscreen has become a special consideration in patients with AD.[21] Since silica nanoparticles have been used in sunscreen and various cosmetics.[22] These nanoparticles are absorbed through the skin and interact with other materials, which potentially aggravates AD.[23]

TiO_2 nanoparticles in cosmetics, toothpaste, and sunscreen can penetrate the human stratum corneum and some hair follicles but not the deep layers of the skin.[24] However, a study demonstrated that silica nanoparticles that were 70 nm in diameter can penetrate the skin barrier and can be recognized by keratinocytes and antigen-presenting cells.[4] Recent studies indicate that the epidermal permeability barrier plays a crucial role in AD, which is closely correlated with chronic immune reactions in the skin during systemic allergic responses.[16,25] Therefore, it is possible that silica nanoparticles may be associated with the development of allergic diseases such as AD; however, the effect of pore structural conditions of silica nanoparticles on AD symptoms has not been fully elucidated.

Mesoporous silica nanoparticles (MSN) are designed to exhibit greater pore volumes and surface areas and a more ordered pore structure than amorphous colloidal silica nanoparticles (CSN).[26] High-reactivity pore structures considerably influence biological responses.[27,28] The pore structures of nanomaterials are considered a key factor in the induction of nanotoxicity owing to their different efficiencies in cellular uptake and immune response generation.[26] We previously reported that in vivo exposure to MSN caused more damage to the systemic immunity than exposure to CSN, by assessing immunotoxicity in the spleen.[29] However, despite the increasing cutaneous application of MSNs owing to their high surface area, the effect of the surface area of silica amorphous colloidal silica nanoparticles on allergic inflammation such as AD is not completely understood. In this study, we conducted a comparative analysis of two types of silica nanoparticles (MSN and CSN) and their plasma-protein adsorption. The protein-corona formation in silica nanomaterials, which can induce immunotoxicity, may vary depending on the surface structure. In addition, we compared the effects of two types of silica protein corona on claudin-1 to explain their adverse effects on the severity of AD symptoms. The immunotoxic effect of plasma-protein adsorption was comprehensively investigated in different mouse models of AD-like skin inflammation.

Materials and Methods

Nanoparticle Preparation

CSN and MSN (MCM41 type) were provided by Orion High Technologies (Spain). CSN and MSN were prepared using similar processes, except for the addition of the ionic surfactant CTAB as a template for MSN. The MSNs were prepared using dilute TEOS and a low surfactant concentration, as follows: 0.66 g of CTAB was dissolved in a mixture of distilled water (800 mL) and ammonium hydroxide (26.4 mL, 29 wt% NH_3 in water); 3 mL of TEOS was carefully added with vigorous stirring. The precursor solution was stirred for 3 h at room temperature. To remove the surfactant template, the synthesized MSNs were refluxed in a solution of HCl (1 mL, 37.4%) and methanol (100 mL), followed by repeated washing with methanol and water (10 times, in general). The surfactant-removed MSNs were placed in ethanol and sonicated before use for preventing amorphous colloidal silica nanoparticle aggregation. CSNs were synthesized by mixing 500 mL of ethanol, 20 mL of distilled water, 20 mL of ammonium hydroxide, and 30 mL of TEOS. The precursor solution was stirred for 24 h, filtered, washed with water, and re-dispersed in ethanol.

Physiochemical Characterization of Silica Nanoparticles

The zeta potential and hydrodynamic sizes of each nanoparticle were analyzed in distilled water using a zeta sizer (Litesizer™ 500, Anton Paar, Austria). The morphological and elemental analyses of mesoporous silica nanoparticles (MSNs) and colloidal silica nanoparticles (CSNs) were performed using transmission electron microscopy (TEM Technai G2 F30 S-Twin, FEI company, USA). The silica nanoparticles were dispersed in distilled water and deposited on a carbon grid for air-drying the solution for one day before TEM analysis. All TEM images were obtained at 300 kV. To determine the specific surface area and pore volume, nitrogen physisorption analysis was performed at −195.8 °C using Micromeritics' Tristar II 3020 equipment (Micromeritics Instrument Corporation, USA). Prior to measurement, all samples were degassed under vacuum at 95 °C for 14 hrs. The pore size distribution was calculated using Barrett-Joyner-Halenda (BJH) Analysis.

Protein Absorption and BSA Blocking of Silica Nanoparticles

CSN and MSN were quantified (0.5, 1, 5, and 10 mg) for each experimental group, placed in tubes, and dissolved in 50% FBS in PBS through sonication. The mixture was stirred using a stirrer in a 37°C incubator, and the reaction was allowed to proceed for 6 h. The supernatant was removed by centrifugation at 13,000 rpm for 10 min, and FBS that was not absorbed was removed by washing. The samples were prepared by dissolving MSN and CSN pellets that absorbed FBS in PBS. Samples were prepared under the same conditions as used for the negative control, which contained only FBS without silica nanoparticles. Blocking was performed using bovine serum albumin (BSA), after which silica was dissolved in 5% BSA in PBS and gently shaken for 1 h. Next, the absorbed protein was quantified using the Bradford assay kit (23,236, Thermo Fisher Scientific, Waltham, MA, USA) following the manufacturer's protocol. The samples with 0.5 mg and 1 mg of nanoparticles was estimated to contain 1–25 μg of protein and in samples with 5 mg and 10 mg, 100–1500 μg of protein. The amount of protein absorbed by the CSN and MSN was quantified using spectroscopy at a wavelength of 595 nm. Subsequently, CSN and MSN samples with absorbed proteins were centrifuged, and the pellets were released in 21 μL of distilled water. The samples were prepared for SDS-PAGE analysis by the addition of 7 μL of 4X Laemmli's SDS-sample buffer (L1200, GenDEPOT, Katy, TX, USA). The samples were boiled at 95°C for 5 min and centrifuged at 13,000 rpm for 1 min. The supernatant was electrophoresed at 80–100 V on a 0.75 mm-thick SDS-PAGE gel containing 10% acrylamide and the gel stained with Coomassie blue. The positive controls, that is, 30 μg of FBS, BSA, and a mixture of FBS and BSA, were prepared in a similar manner as the samples and electrophoresed.

Cell Culture

The HaCaT human keratinocyte cell line was purchased from CLS Cell Lines Service (Eppelheim, Germany). Cells were maintained in Dulbecco's modified Eagle's medium (DMEM) supplemented with 10% FBS and antibiotics (100 U mL^{-1} penicillin G and 100 μg mL^{-1} streptomycin) at 37°C in 5% CO_2.

Uptake Analysis of Silica Nanoparticles by Confocal Microscopy

HaCaT cells were seeded (5×10^4 cells) on poly-D-lysine-coated coverslips and cultured overnight. The cells were pre-incubated with different inhibitors at various concentrations (ie, 5-(N-ethyl-N-isopropyl) amiloride (EIPA, 50 μM), chlorpromazine (CPZ, 20 μM), or genistein (GEN, 200 μM, Sigma) for 1 h at 37°C to inactivate the micropinocytosis, caveolin-mediated, and clathrin-mediated pathways, respectively. Next, CSN-Alexa 488 or MSN-Alexa 488 was added to the cells and incubated for 6 h at 37°C following which, all samples were fixed with 4% paraformaldehyde in medium overnight at 4°C. The fluorescence signals from the treatment groups were evaluated at the same setting, using confocal microscopy LSM700 (Carl Zeiss, Germany).

Immunofluorescence and Confocal Microscopy

HaCaT cells were grown on chamber slides and treated with 500 μg mL^{-1} CSN, MSN, inactivated protein corona-CSN, or inactivated protein corona-MSN for 12 h. The cells were fixed, blocked with 10% BSA, and incubated with primary antibodies against claudin-1 (Abcam). The slides were washed, incubated with Alexa Fluor 488-conjugated secondary antibodies (Invitrogen) and DAPI, and examined using a laser scanning confocal microscope (LSM800; Carl Zeiss).

Animals

Six-week-old female BALB/c mice were purchased from SLC Inc. (Hamamatsu, Japan). Five mice were housed per cage in a laminar air flow room maintained at a temperature of 22 ± 2°C and a relative humidity of 55 ± 5% throughout the study. The care and treatment of the mice were in accordance with the guidelines established by the Public Health Service Policy on the Humane Care and Use of Laboratory Animals and were approved by the Institutional Animal Care and Use Committee. All animal experiments were approved by the Institutional Animal Care and Use Committee of Kyungpook National University (KNU-2020-00501).

Induction of AD-Like Skin Inflammation in the Mouse Ear

The induction of AD using DFE was performed on the basis of our previous research.[30] The mice (n = 5) were divided into six groups, and the surfaces of both ear lobes were stripped very gently three times with surgical tape (Nichiban, Tokyo, Japan). Next, DFE (20 μL, 10 mg mL^{-1}, dissolved in PBS plus 0.5% Tween 20, Greer laboratory Inc., Lenoir, NC, USA) was painted on each mouse ear twice a week for 3 weeks. One week after the initial treatment with DFE, which induced AD-like skin inflammation, the mouse ears were treated twice per week with CSN and MSN (100 or 500 μg per ear) by painting for the duration of the 3-week DFE treatment. Ear thickness was measured 24 h after DFE application using a dial thickness gauge (Mitutoyo, Co., Tokyo, Japan).

On day 21, the mice were euthanized with carbon dioxide. Whole blood samples were collected from the celiac artery. The serum was stored at −70°C for further analysis. Subsequently, the ears were removed and histopathological analysis was performed. Total serum IgE and IgG2a levels were measured using an ELISA kit (BD Biosciences, Oxford, UK) according to the manufacturer's instructions. For the detection of DFE-specific IgE, mite extract (10 mg) was coated in 96-well plates, and the DFE-specific IgE level was assessed by measuring the optical density of each well.

Histological and Immunohistochemical Analysis

The ears were fixed with 4% formaldehyde and embedded in paraffin, and 5 μm sections were stained with hematoxylin and eosin (H&E). Infiltrated lymphocytes, epidermal thickening, and dermal fibrosis were observed under a microscope. For measurement of mast-cell infiltration, the skin sections were stained with toluidine blue, and mast cells were counted at five random sites. Eosinophils were counted in a blinded manner in 10 high-power fields at a magnification of 400×. Dermal thickness was analyzed in H&E-stained sections (100× magnification). Thickness was measured in five randomly selected fields from each sample.

Histamine Assay

Histamine content was measured using the *o*-phthaldialdehyde spectrofluorometric procedure.[31] The collected blood was centrifuged at 400 ×g for 10 min, and the serum was withdrawn for measuring histamine content. Fluorescence intensity was measured using 355 nm excitation and 450 nm filters on an LS-50B fluorescence spectrometer (Perkin-Elmer, Norwalk, CT, USA).

FACS Analysis

Both auricular LNs were collected from each mouse and ground using 70 μm nylon cell strainers (Falcon, Bedford, MA, USA) for isolation of single cells. Subsequently, the cells were stained using mouse CD4 PerCP-Cy™5.5-FITC-conjugated Th1 (IFN-γ), CD4 PerCP-Cy™5.5-APC-conjugated Th2 (IL-4), and CD4 PerCP-Cy™5.5-PE-conjugated Th17 (IL-17A) phenotyping kit (BD Biosciences). Fluorescence intensity was detected using a FACSCalibur flow cytometer (BD Biosciences).

Quantitative Real-Time Polymerase Chain Reaction

For measuring cytokine expression, quantitative real-time PCR was performed using a Thermal Cycler Dice TP850 (Takara Bio Inc., Shiga, Japan) according to the manufacturer's protocol. At the end of the in vivo experimental period, the ears were excised and total RNA was isolated. The HaCaT cells were treated with 100 or 500 μg mL^{-1} MSN or CSN, respectively, for 6 h. Total cellular RNA was isolated from the cells (2×10^5 cells per 24-well plate).[30] Briefly, cDNA (2 μL, 100 ng), sense and antisense primer solution (1 μL, 0.4 μM), SYBR Premix Ex Taq (12.5 μL, Takara Bio Inc.), and dH_2O (9.5 μL) were mixed to obtain a final reaction mixture (25 μL) in each reaction tube. The PCR conditions were similar to that described in a previous study.[30] mRNA expression was normalized and quantified using the TP850 software, supplied by the manufacturer.

Western Blotting

The ears were excised after day 21 of AD induction and homogenized in radioimmunoprecipitation assay buffer supplemented with a protease inhibitor cocktail (Sigma). The proteins were electrophoresed on a 10% SDS-PAGE gel and transferred onto nitrocellulose membranes. The membranes were stained with reversible Ponceau S to ensure equal loading of the samples in the gel. After blocking for 1 h with 5% w/v dry milk powder in Tris-buffered saline with Tween 20 buffer, the membranes were incubated overnight with claudin-1 antibodies (Abcam). Immunodetection was performed using SuperSignal West Pico Chemiluminescent Substrate (Thermo Fisher Scientific). β-Actin was used as the loading control.

Statistical Analysis

Statistical analyses were performed using Prism 7 (GraphPad Software, San Diego, CA, USA). The treatment effects were analyzed using one-way analysis of variance, followed by Tukey's multiple comparison test. The asterisks denote P values (*$P < 0.05$, **$P < 0.01$, ***$P < 0.001$).

Results

Physicochemical Characterization of Silica Nanoparticles

The hydrodynamic sizes and zeta potentials of CSN and MSN were not significantly different, which indicates that both CSN and MSN share similar physiochemical properties (Figure 1A–C). TEM images of CSN and MSN indicated that both nanoparticles showed the same morphology (spherical), with diameters of 120–160 nm (Figure 1A). The atomic elemental compositions of CSN and MSN were measured by EDS mapping; the results confirmed that both CSN and MSN mainly consisted of silicon and oxygen (Figure 1A). The elemental compositions of the nanoparticles were quantitatively analyzed using X-ray photoelectron spectroscopy (XPS), and similar to that of EDS mapping, CSN and MSN share not only identical elemental compositions but also similar atomic percentages (Figure 1B). In addition, electron spectroscopy (ESCA) for chemical analysis was performed on the O1s, C1s, and Si2p peaks for comparing the comparative regions of each curve representing the atomic weight ratio; the results were similar for CSN and MSN (Supplementary Figure 1A). The CSN size was distributed from 77 nm to 200 nm (mean size: 130 nm), while the MSN size was distributed from 98 nm to 220 nm (mean size: 160 nm), which was slightly larger than that of CSN (Figure 1C). The polydispersity index (PDI) was less than 0.3 in all test samples (Supplementary Figure 1B). Evaluation of the surface structure of CSN and MSN showed significant differences in surface area and pore volume, confirming that the surface of MSN had a porous structure (Figure 1D). The specific surface area assessment was obtained using the Brunauer-Emmett-Teller (BET) equation, which is presented in Supplementary Figure 2A. For detailed information on the surface area, pore volume, and pore size of MSNs by Brunauer-Emmett-Teller (BET) analysis, please see Supplementary Table 1 and Supplementary Figure 2B–C). Despite the chemical similarities between CSN and MSN, MSN could favorably form protein-corona by inducing greater plasma protein adsorption than CSN owing to its highly porous structures and surface area (Figure 1E–F). Protein adsorption on the surface of MSN, according to electrophoresis analysis, was greater than that on CSN in an FBS environment, which mimics the blood-contact conditions (Figure 1E and F).

Silica-Corona Formation by FBS and Blocking Corona by BSA Adsorption

To inhibit the potential cellular functions of plasma protein coronas adsorbed on CSN and MSN surfaces, bovine serum albumin (BSA) was allowed additionally to be adsorbed on the surfaces of CSN and MSN (Figure 2A–F). FBS corona formation increased the size of CSN by 80 nm relative to the size of free-CSN (average size 120 nm), and CSN with adsorbed BSA was 50 nm larger than CSN with FBS-corona formation (Figure 2A and B). In addition, FBS corona formation increased the size of MSN by 100 nm relative to the size of free-MSN (average size 260 nm), and MSN with adsorbed BSA was 60 nm larger than MSN with FBS-corona formation (Figure 2D and E). TEM images showed that CSN and MSN reacted with FBS to form a protein corona and that the protein-corona formation was inhibited through BSA adsorption (Figure 2C and F). In addition, using electrophoresis, the BSA adsorption of CSN-corona and MSN-corona was analyzed and confirmed on the basis of the amount and size of the protein (Figure 2G).

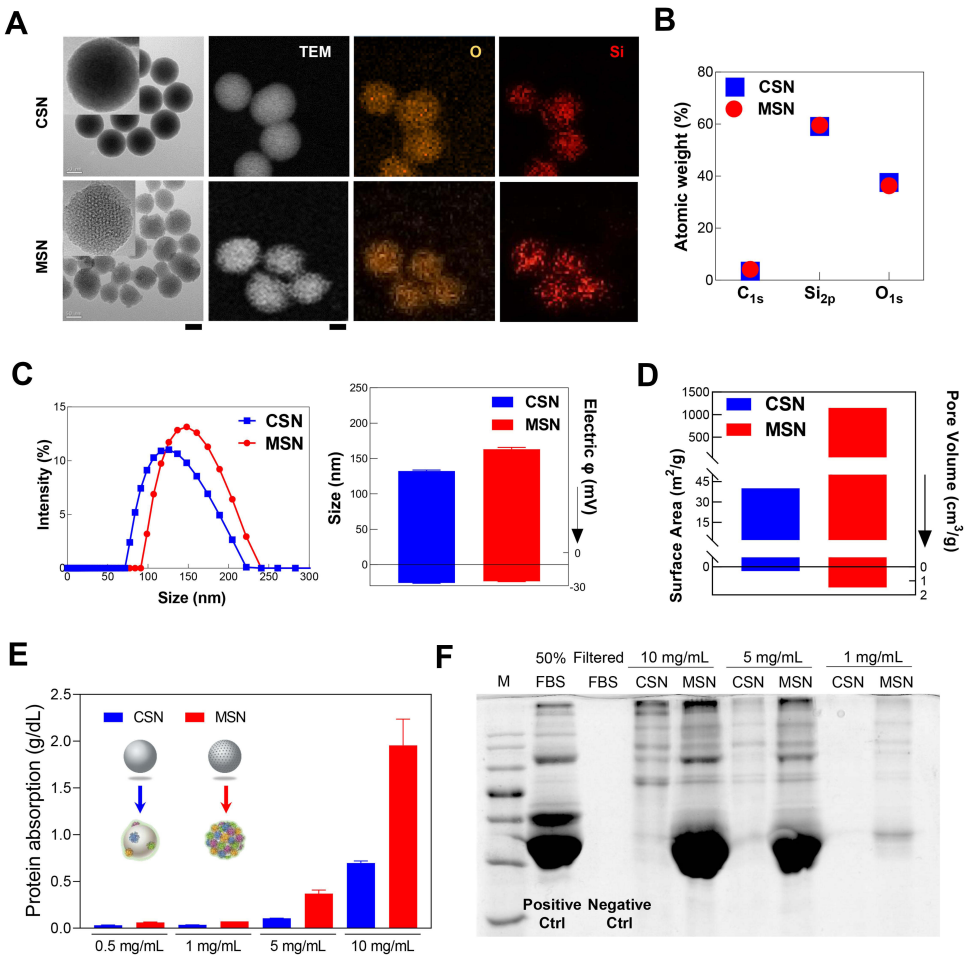

Figure 1 Physicochemical properties of CSN and MSN (**A**) TEM images and EDS mapping of MSN and CSN. The scale bar is 50 nm. (**B**) XPS analysis of MSN and CSN showing identical surface atomic elements. (**C**) Size distributions of MSN and CSN showing identical sizes on the nanoscale. The mean size and electrical potential of MSN and CSN are identical. (**D**) MSN show greater surface areas due to increased porosity than CSN. (**E**) Capacity of FBS protein adsorption according to CSN and MSN concentration. (**F**) Electrophoretic bands of CSN and MSN reacted with proteins in FBS.

Keratinocyte Uptake Analysis

The cellular uptake analysis demonstrated that cellular uptake strongly depends on the protein-corona formation surrounding nanoparticles.[32,33] Because of the increased amount of adsorbed proteins, MSN-corona exhibited a greater uptake efficacy than the non-porous CSN-corona (Figure 3A–E). Specifically, through confocal microscopy, we evaluated the intracellular uptake of two different surface structures (CSN and MSN), streptavidin-Alexa 488-embedded CSN-corona and MSN-corona (Alexa-CSN-corona and Alexa-MSN-corona, respectively) by human keratinocytes (HaCaT); the confocal microscopy images were obtained and analyzed after 6 h of incubation. MSN-corona exhibited a significantly higher uptake by HaCaT cells than CSN-corona (Figure 3A and C). To investigate specific intracellular uptake channels in HaCaT cells, we used inhibitors of micropinocytosis (amiloride, EIPA), clathrin-mediated endocytosis (chlorpromazine, CPZ), and caveolae-mediated endocytosis (genistein, GEN) to identify the endocytic mechanism responsible for the uptake of MSN-corona. The uptake of plasma protein-adsorbed MSN was strongly dependent on caveolae-and clathrin-mediated endocytosis pathways in HaCaT cells (Figure 3B and D). In conclusion, greater protein corona adsorption by MSN resulted in increased MSN uptake through caveolae and clathrin mediated endocytosis of keratinocytes (Figure 3D and E).

Inhibition of Cellular Uptake of MSN Corona by BSA Adsorption

A previous study confirmed that BSA or HSA adsorption on nanoparticles reduced the intracellular uptake and delivery of these nanoparticles to the lysosomes.[34] The adsorption of BSA alone on nanoparticles decreases their adhesion to cell membranes,

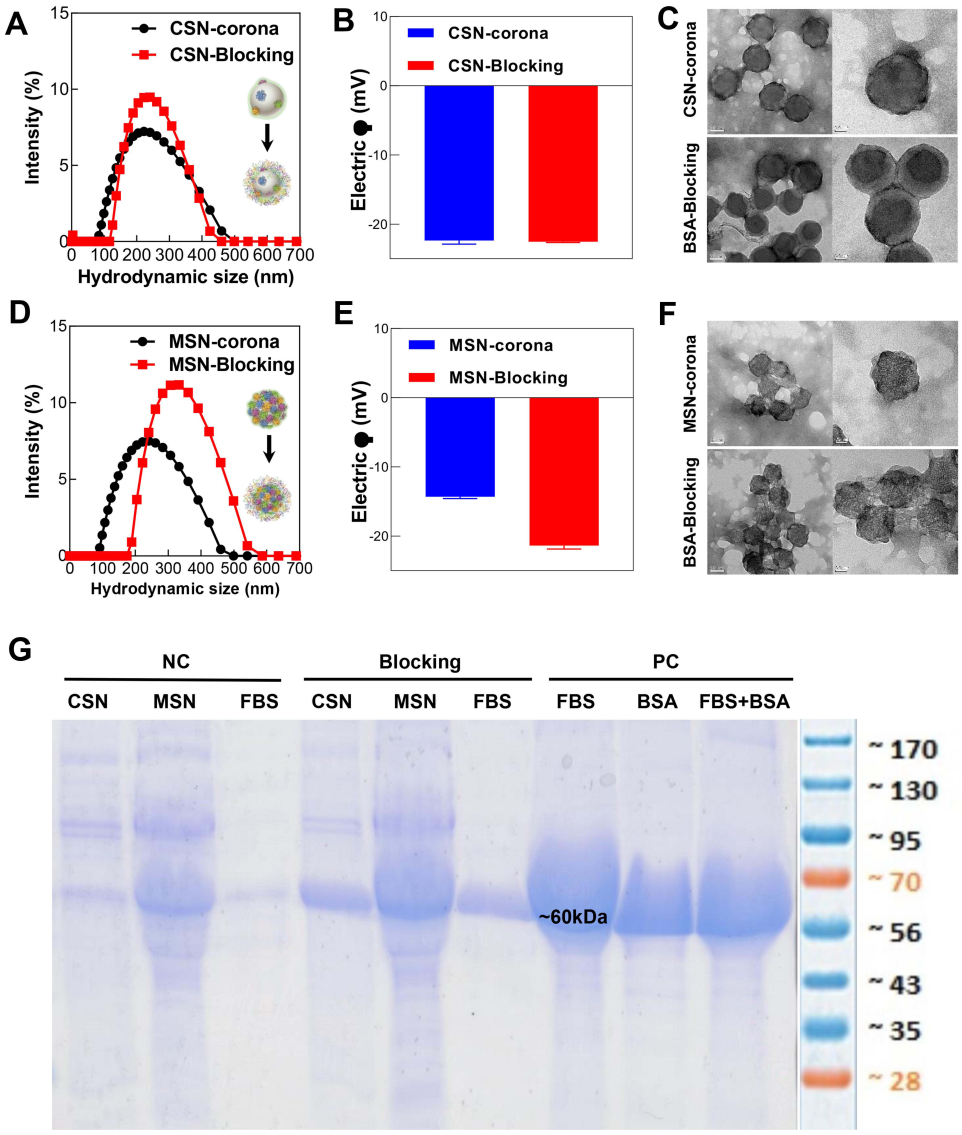

Figure 2 Physicochemical properties of Silica-Corona and BSA adsorption on Silica Corona. (**A**) Size distributions of CSN-FBS and BSA-blocked CSN show identical sizes in the nanoscale. (**B**) The electric potential of CSN-FBS and BSA-blocked CSN are identical. (**C**) TEM images show CSN Corona and additional adsorption of BSA on CSN Corona. The scale bar is 50 nm. (**D**) Size distribution of MSN-FBS and BSA-blocked MSN showing identical sizes in the nanoscale. (**E**) The electric potential of MSN-FBS and BSA-blocked MSN are identical. (**F**) TEM images show MSN Corona and additional adsorption of BSA on MSN-Corona. The scale bar is 50 nm. (**G**) Electrophoretic bands of CSN-Corona and MSN-Corona deactivated with BSA coating.

resulting in decreased cellular uptake.[35] These results provide evidence that the use of BSA on a silica-protein corona can prevent intracellular absorption. We observed that the MSN corona, which induced considerable intracellular absorption in HaCaT cells, was not uptake intracellularly after the corona was blocked with BSA (Figure 4A–C). Confocal images showing intracellular uptake of MSN-corona and BSA-adsorbed MSN were obtained and analyzed after 6 h of incubation; they confirmed that BSA-adsorbed MSN showed significantly lower uptake in HaCaT cells than MSN-corona (Figure 4A and B). In conclusion, additional adsorption of BSA on the MSN protein corona inhibited their uptake by keratinocytes (Figure 4C). Therefore, it is proved that the difference in the formation of protein corona, according to the surface structure of silica nanoparticles, is the most important factor that causes the difference in absorption by skin cells (Figure 4C).

Plasma-Adsorbed MSN Induces the Disruption of Claudin-1

The interaction of the protein corona with nanoparticles can result in biological barrier disruption and, eventually, cell death.[36] Claudin-1 is a transmembrane protein of a complex epidermal barrier system that prevents external antigen penetration;

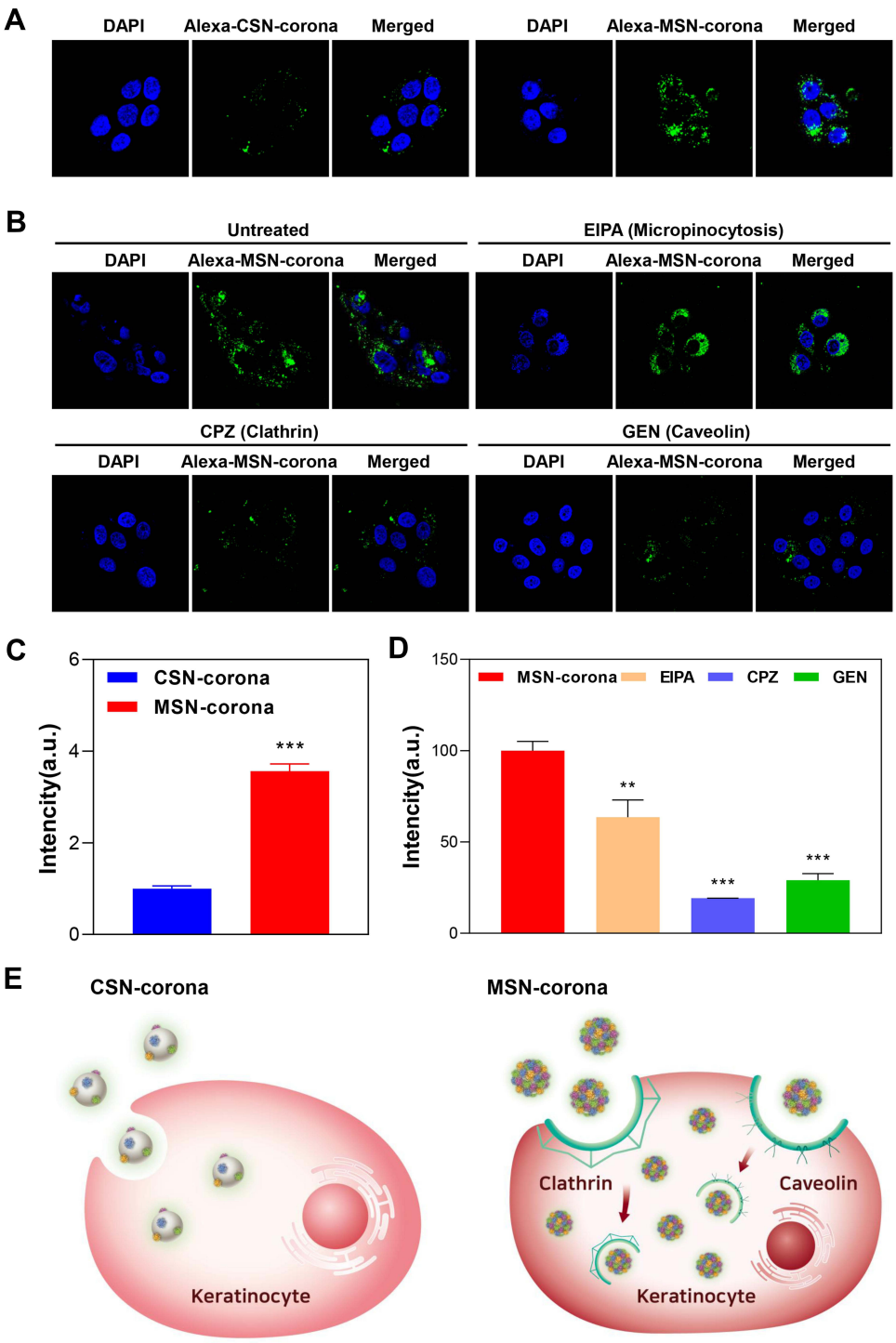

Figure 3 Cellular uptake of CSN and MSN in keratinocytes. (**A**) HaCaT cells treated with Alexa-CSN-Corona and Alexa-MSN-Corona showing different cellular uptake intensities after 6 h. (**B**) HaCaT cells pretreated with inhibitors of micropinocytosis (EIPA), clathrin-mediated endocytosis (CPZ) and caveolae-mediated endocytosis (GEN), showing that MSN-Corona uptake is mediated by clathrin and caveolin endocytosis after 6 h. (**C**) Florescence intensity (uptake) analysis of TNF-α- and IFN-γ-stimulated HaCaT treated with CSN-Corona or MSN-Corona. (**D**) Florescence intensity (uptake) analysis of TNF-α- and IFN-γ-stimulated HaCaT treated with MSN and inhibitor. (**E**) Schematic illustration of the difference between CSN-Corona and MSN-Corona uptake in HaCaT cells. The data are presented as the mean ± SD. $^{**}P < 0.01$ and $^{***}P < 0.001$.

reduced claudin-1 is correlated with various inflammatory reactions in human and mouse AD.[37] Exposure of epithelial cells to proinflammatory cytokines affects changes in the composition and barrier function of tight claudins.[38,39] To test whether the two types of nanoparticles can directly affect changes to claudin-1, which is part of the skin barrier and inflammatory

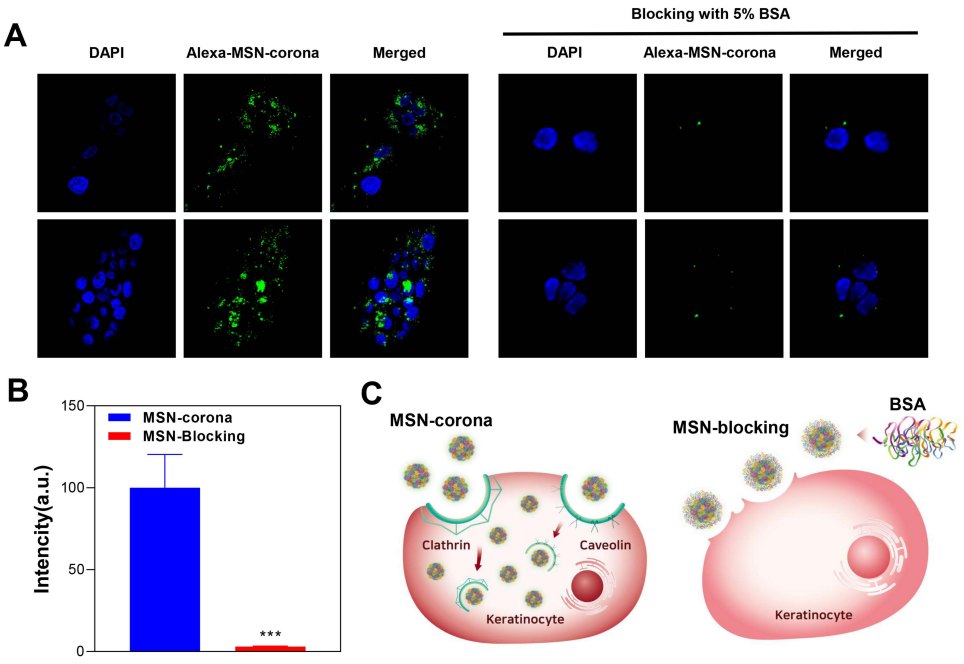

Figure 4 Cellular uptake of BSA-adsorbed MSN in keratinocytes. (**A**) HaCaT cells treated with MSN-Corona and BSA-blocked MSN-Corona, showing different cellular uptake intensities after 6 h. (**B**) Florescence intensity (uptake) analysis of TNF-α- and IFN-γ-stimulated HaCaT treated with MSN-Corona and BSA-adsorbed MSN. (**C**) Schematic illustration of the difference in intracellular uptake of the MSN-protein Corona and MSN-protein Corona blocked by BSA adsorption in HaCaT cells. The data are presented as the mean ± SD. ***$P < 0.001$.

responses when absorbed into keratinocytes in vitro, we stimulated HaCaT cells with BSA-adsorbed protein-corona-inactive nanoparticles, normal nanoparticles, and TNF-α/IFN-γ (control group to induce an AD-like condition in keratinocytes) for 12 h and subsequently analyzed the cells using qPCR and confocal microscopy. Claudin-1 was detected in large amounts in untreated and CSN-treated HaCaT cells. However, claudin-1 levels were significantly reduced in MSN-treated cells, as well as in TNF-α/IFN-γ-treated cells. BSA-adsorption-induced inactivation of the protein corona surrounding MSN did not cause disruption of claudin-1 (Figure 5A and B). We further showed that MSN was involved in the production of proinflammatory cytokines (Supplementary Figure 3), reducing claudin-1 levels in keratinocytes. Our data show that the adsorption of protein corona onto the porous surface of MSNs is greater than that onto non-porous CSNs, leading to increased absorption of MSN into keratinocytes and enhanced production of proinflammatory cytokines. These results suggest that MSN can be absorbed into keratinocytes through the formation of a large amount of protein corona, producing proinflammatory cytokines and impairing claudin-1 function. In AD, the downregulation of claudin-1 is greatly affected by dermal inflammation. We next evaluated whether nanoparticles contributed to the destruction of claudin-1 in normal and AD mouse models. The expression of claudin-1 in the ear tissues of *D. farinae* extract (DFE)-induced AD mice treated with MSN or CSN was analyzed by Western blotting. Our results showed that claudin-1 was downregulated in AD skin lesions compared to that in healthy mouse skin. The DFE group treated with plasma-adsorbed MSN exhibited significantly reduced claudin-1 expression in the ear tissue than the DFE-only group, whereas the CSN-treated DFE group showed no changes (Figure 5C). These results provide direct evidence that plasma-adsorbed MSN penetrates the skin and impairs claudin-1 function.

Topical Application of MSN Does Not Affect Normal Mouse Skin

Once nanoparticles enter various organs and are exposed to biological fluids such as blood, non-specific proteins attach to the nanoparticle surface to form a protein corona.[15] Recently, it was reported that the nanoparticle-protein corona complex can mediate innate or adaptive immune responses that affect the immune system.[14] On the basis of the inflammatory responses of human keratinocytes induced by MSN protein corona interactions, we first sought to characterize nanoparticles associated with immune reactions in normal mouse skin and explore their potential to induce

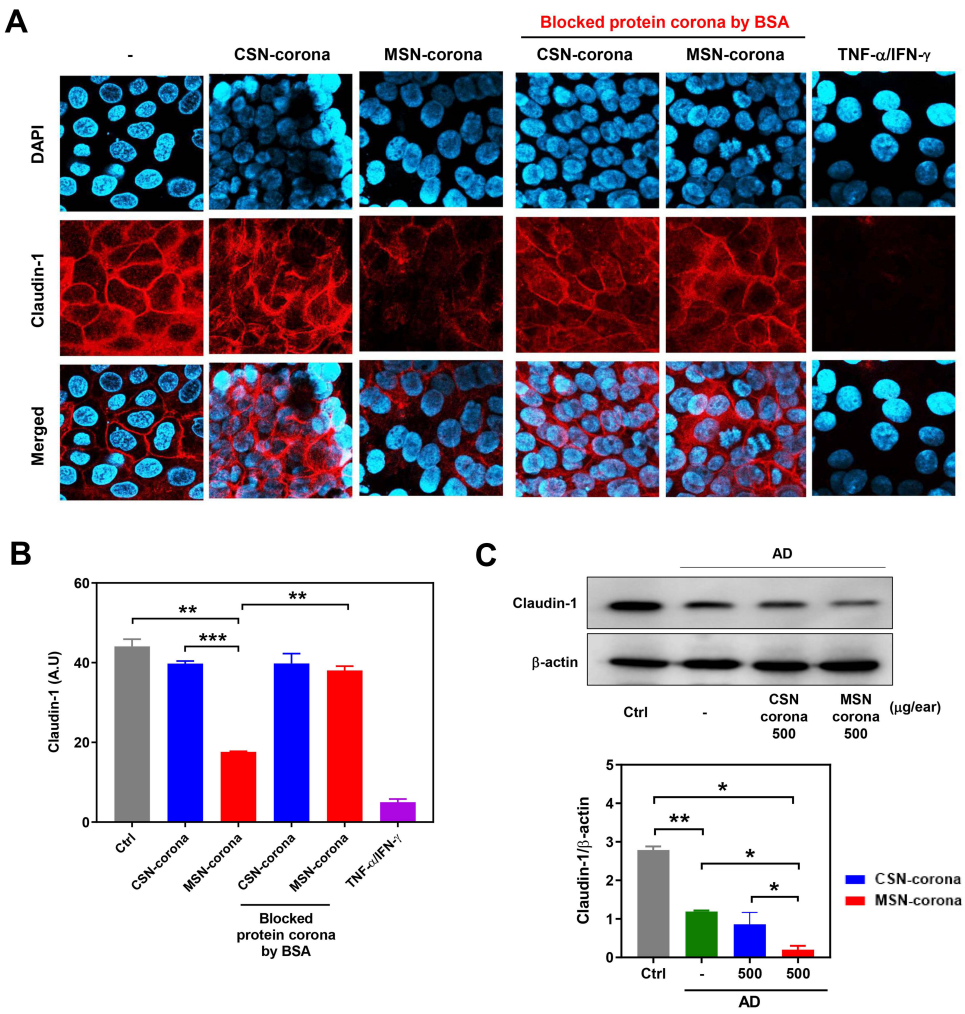

Figure 5 MSN-Corona can induce the disruption of claudin-1. (**A**) HaCaT cells were treated with CSN-Corona, MSN-Corona, inactivated protein Corona-CSN, or inactivated protein Corona-MSN for 12 h. Cells were fixed and stained with DAPI prior to visualization of subcellular localization of claudin-1 (red) or nuclei (blue) using immunofluorescence analysis on a laser confocal microscope. Confocal image shows that damage to claudin-1 does not occur in the group treated with BSA-blocked MSN Corona. (**B**) Quantification of immunofluorescence for claudin-1. TNF-α and IFN-γ were used as positive controls. (**C**) To examine claudin-1 expression in CSN- or MSN-treated AD mice, the ears were excised on day 21. Whole cell lysates were analyzed using Western blotting (top). The claudin-1 expression levels were normalized to that of β-actin and quantified using the Image J software (bottom). The data are presented as the mean ± SD of three determinations. $^{*}P < 0.05$, $^{**}P < 0.01$, $^{***}P < 0.001$.
Abbreviations: AD, DFE-induced atopic dermatitis; CSN, colloidal silica nanoparticles; MSN, mesoporous silica nanoparticles.

AD development. We applied low levels of mechanical stress (ear hair removal level) by tape stripping on the ears of healthy BALB/c mice and subsequently topically applied CSN-corona, MSN-corona, or DFE twice per week for a total duration of 21 days (Figure 6A). During the treatment period, ear thickness was measured 24 h after each treatment. DFE-treated AD mice showed characteristic features of severe AD-like skin symptoms, including enlarged epidermis and dermis (Figure 6B), increased ear thickness (Figure 6C), high levels of total serum IgE (Figure 6D), and DFE-specific IgE (Figure 6E). However, topical application of neither MSN-corona nor CSN-corona induced AD skin inflammation from normal skin, similar to the effect of DFE treatment. These results suggest that in normal skin, the tight junction of the epidermis works as a skin barrier to stop MSN and CSN from entering the dermis, thereby preventing them from inducing dermatitis (Figure 6F).

MSN-Corona Exacerbates AD-Like Skin Inflammation Compared with CSN-Corona

Our next aim was to validate the variable of the two types of silica nanoparticle-corona on AD conditions. DFE was topically applied to the ears of BALB/c mice; both MSN-corona and CSN-corona were topically applied twice per week

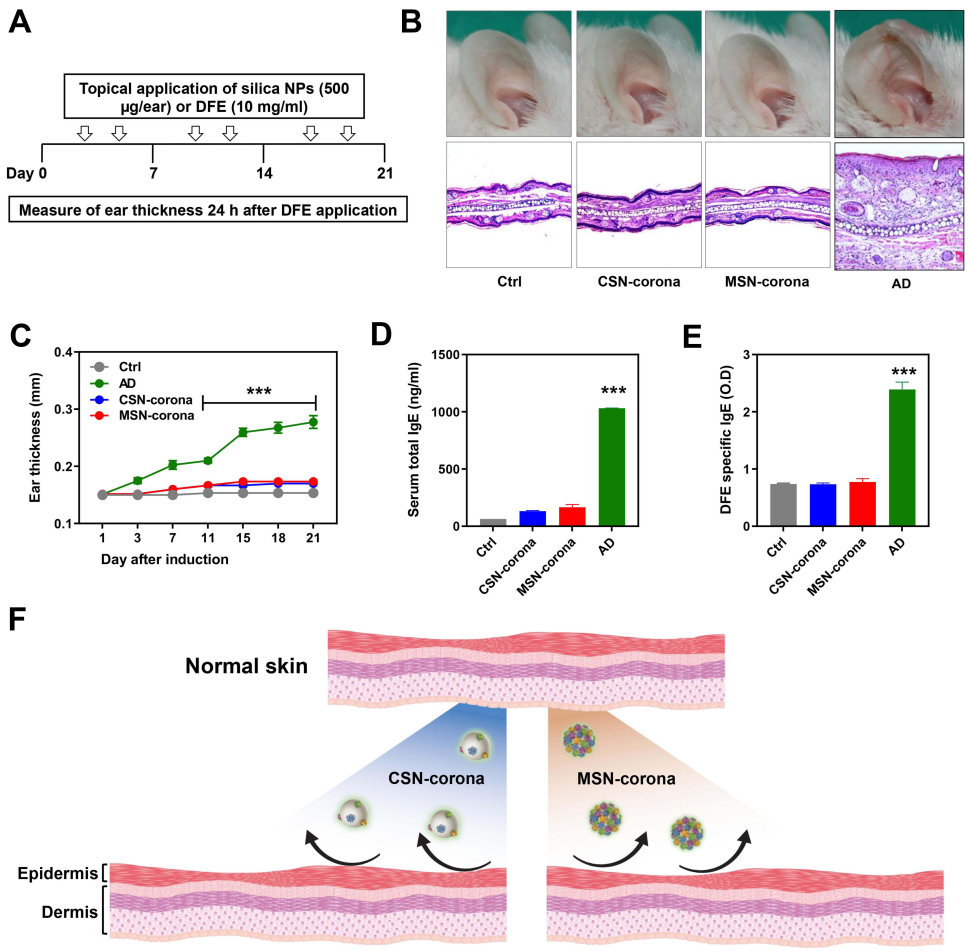

Figure 6 Topical application of CSN-Corona and MSN-Corona does not affect healthy mouse skin. (**A**) The experimental scheme for topical application of CSN-Corona, MSN-Corona, or DFE. CSN-Corona, MSN-Corona, or DFE was applied six times for three weeks (n = 5). (**B**) Representative photomicrographs of ear sections stained with hematoxylin and eosin (H&E, scale bar = 40 μm). (**C**) Ear thickness was measured 24 h after CSN-Corona, MSN-Corona, or DFE application with a dial thickness gauge. Serum total IgE (**D**) and DFE-specific IgE (**E**) levels were measured using ELISA. (**F**) Schematic illustration of normal skin tissues upon MSN and CSN treatment. The data are presented as the mean ± SD. ***$P < 0.001$ compared with the control.

Abbreviations: AD, DFE-induced atopic dermatitis; CSN, colloidal silica nanoparticles; MSN, mesoporous silica nanoparticles.

for 21 days after AD induction (Figure 7A). The ear thickness in each group was similar until day 11. MSN-corona and CSN-corona treatment of DFE-treated mice caused a notable increase in ear thickness after 18 days (Figure 7B). The MSN-corona treatment significantly increased the ear thickness relative to the CSN treatment.

Microscopic analysis of the ear skin revealed several histologic alterations after DFE treatment, including hyperkeratosis and inflammatory cell infiltration (Figure 7C). Histopathological analysis revealed a significant difference in the effects of MSN-corona treatment and CSN-corona treatment in DFE-treated mice. Epidermal (Figure 7D, left panel) and dermal thicknesses (Figure 7D, middle panel), as well as eosinophil infiltration (Figure 7D, right panel), were significantly higher in the former than in the latter. Mast cells are essential effector cells that serve as a primary source of symptom-inducing histamine in AD.[16] Inflammatory mediators and histamine released from mast cells contribute to itching and inflammation in AD. As expected, DFE-treated AD mice displayed enhanced mast cell infiltration and increased serum histamine levels (Figure 7C and E). However, the DFE group treated with MSN-corona exhibited a greater increase in these measures than the DFE-only group. In addition, MSN-corona treatment significantly increased mast-cell infiltration (Figure 7E, left panel) and histamine secretion (Figure 7E, right panel) compared to CSN-corona treatment, following a high dose (500 μg per ear) application. These results indicate that, unlike in normal mice, greater amounts of protein coronas were adsorbed onto the porous MSN surface in the biological fluid of the AD mice. These fluids include secreted factors from inflammatory cells, blood, and wound discharge in the ear tissue of AD mice, leading

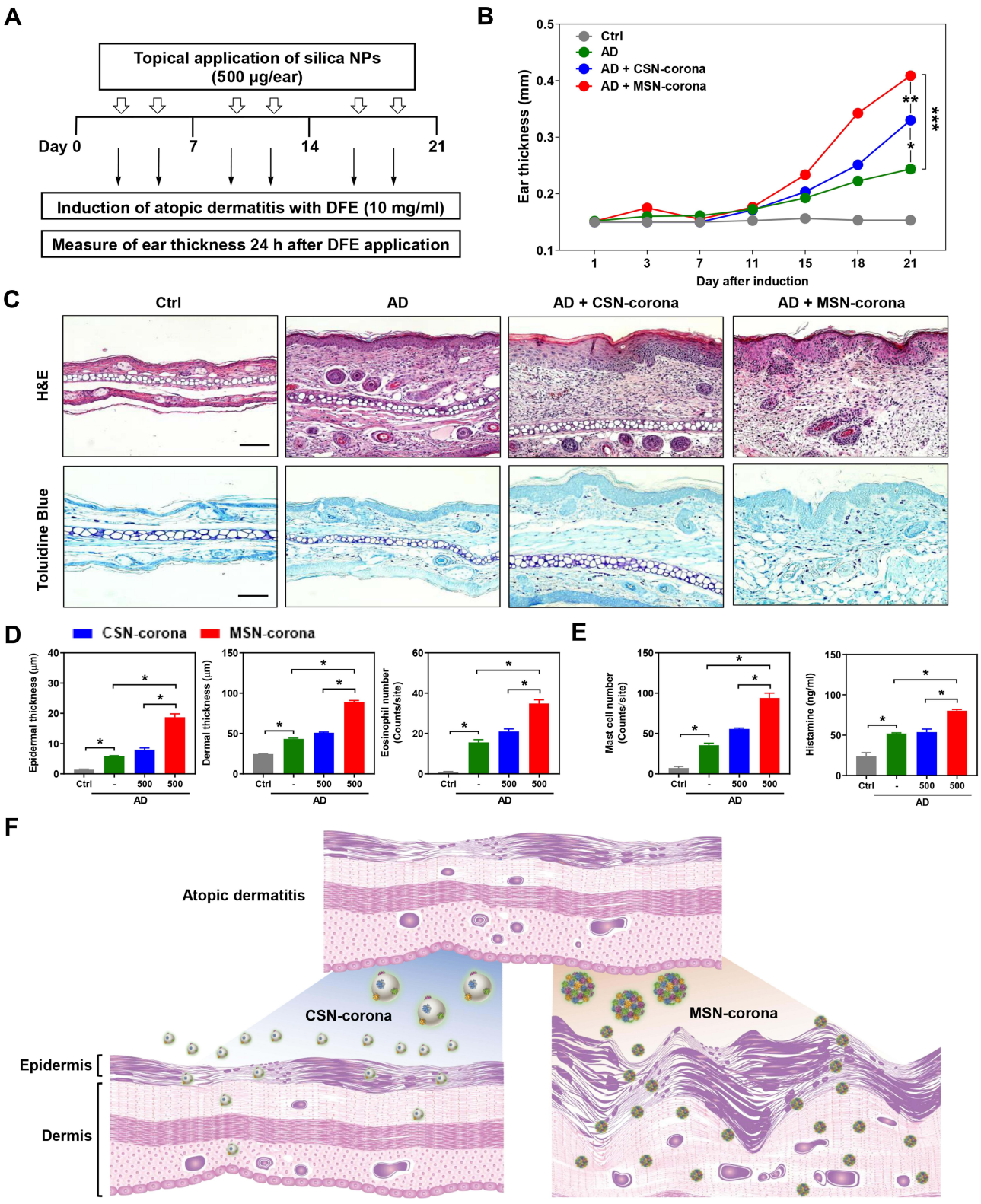

Figure 7 MSN-Corona exacerbate clinical features of AD skin inflammation compared to CSN. (**A**) DFE was applied to both ears twice a week for 4 weeks. CSN-Corona and MSN-Corona were applied six times for 3 weeks (n = 5). (**B**) Ear thickness was measured 24 h after DFE application with a dial thickness gauge. (**C**) Representative photomicrographs of ear sections stained with H&E or toluidine blue (scale bar = 40 μm). (**D**) Epidermal thickness (left), dermal thickness (middle), and number of eosinophils (right). (**E**) Number of mast cells (left) and serum histamine levels (right). (**F**) Schematic illustration of AD skin tissues upon MSN and CSN treatment. The data are presented as the mean ± SD of five determinations. **P* < 0.05, ***P* < 0.01, ****P* < 0.001.

Abbreviations: CSN, colloidal silica nanoparticles; MSN, mesoporous silica nanoparticles.

to the formation of a larger protein corona that can increase epidermal absorption of MSN and affect dermal tissue. Therefore, unlike CSN, MSN coalesces with the atypical proteins, forming a massive corona that further damages the proteins of the epidermal layer; then, MSN enters the dermis and causes changes to the skin tissues that may aggravate dermatitis (Figure 7F).

MSN-Corona Disrupts the AD Mouse Immune System

The acute stage of AD is characterized by the infiltration of Th2 cells, while Th1 cells are detected in the chronic stage. Patients with AD tend to produce high levels of Th2 cytokines, such as IL-4, IL-13, and IL-31, in all stages.[40,41] These cytokines subsequently stimulate B cells to promote the production of IgE antibodies that cause itching, blisters, and inflammation in the epidermis and dermis.[42,43] Th1 cells are characterized by IFN-γ secretion, which induces skin hypertrophy and the proliferation of keratinocytes in the epidermis during the chronic stage.[44] IgE production is related to a predominant Th2 cellular response, whereas IgG2a production is related to the Th1 response.[16] Previous reports have shown a considerable increase in serum Ig levels and the expression of Th2 and Th1 cytokines in DFE-induced AD-like lesions.[45] To discern the role of nanoparticle-corona in Th2 or Th1 cellular responses in AD, we examined the serum levels of IgE (total and DFE-specific) and IgG2a. The MSN-corona-treated DFE group showed significant enhancement in the serum levels of total IgE, DFE-specific IgE (Figure 8A), and IgG2a (Figure 8B) compared to the CSN-corona-treated DFE group.

T cell polarization in AD is biphasic. A predominantly Th2 response is observed in the acute phase, whereas the chronic phase is characterized by a Th1 response.[46] $CD4^+$ T cells can be classified according to their effector cytokines: Th1 (TNF-α and IFN-γ), Th2 (IL-4, IL-13, and IL-31), and Th17 (IL-17A).[47] nanoparticles can induce inflammatory cytokine production by T cells through the adaptive immune system.[36] T cell immune response generally occurs at a compromised site, at which an innate immune reaction is occurring, and enhances the existing inflammatory process occurring in the area. These immune reactions may be directed against the nanoparticles, or they may occur after the formation of a protein corona.[36] Thus, we sought to determine whether the two types of silica nanoparticle-corona could promote the expansion of T lymphocytes, particularly Th1-/Th2-/Th17-phenotype $CD4^+$ T cells, and cytokine production in mice with AD-like skin lesions. The expansion of $CD4^+$ Th1 ($IFN\text{-}\gamma^+$), Th2 ($IL\text{-}4^+$), and Th17 ($IL\text{-}17A^+$) cells in the auricular lymph nodes (LNs) was measured using FACS analysis after 21 days of induction. The MSN-corona-treated DFE group exhibited a significant increase in $CD4^+$ T cells producing $IFN\text{-}\gamma^+$, $IL\text{-}4^+$, and $IL\text{-}17A^+$. A similar increase, but to a lesser degree, was observed in the DFE-only and CSN-corona-treated DFE groups (Figure 8C).

We next investigated the role of the silica nanoparticle-corona in the expression of AD-related inflammatory cytokines in the ear tissue using quantitative real-time PCR. Our results showed that all cytokines were upregulated in the AD-like skin lesions. Consistent with the FACS data, the MSN-corona-treated DFE group showed significant increases in the expression of Th1 (TNF-α and IFN-γ), Th2 (IL-4, IL-13, and IL-31), and Th17 (IL-17A) cytokines compared with the DFE-only and CSN-corona-treated DFE groups following high-dose treatment (500 μg per ear) (Figure 8D). The application of MSN-corona enhanced the production of both Th1 and Th2 cytokines as compared to CSN-corona treatment in the draining LNs and ears (Figure 8C and D). In addition, the cutaneous application of MSN-corona induced Th17 cell response in the draining LNs and ears (Figure 8C and D), suggesting that a Th17 cell response is important for the acute aggravation of AD pathogenesis. Collectively, these results suggest that exposure to MSN-corona over the AD induces a mixed Th1/Th2/Th17-type chronic skin inflammatory response compared to CSN-corona exposure (Figure 8E); application of MSN may negatively modulate T cell immune response to AD.

Discussion

This study demonstrates the effect of protein-corona formation in CSN and MSN by different porous structures and the effect of different types of protein corona on skin inflammation in AD. Our findings indicate that between the MSN and CSN, MSN promotes an increase in plasma protein adsorption, as well as formation of a larger protein corona. MSN disrupts the immune system balance in AD by destroying claudin-1, a tight junction protein in the skin tissue; thus, inducing immunotoxicity and worsening AD.

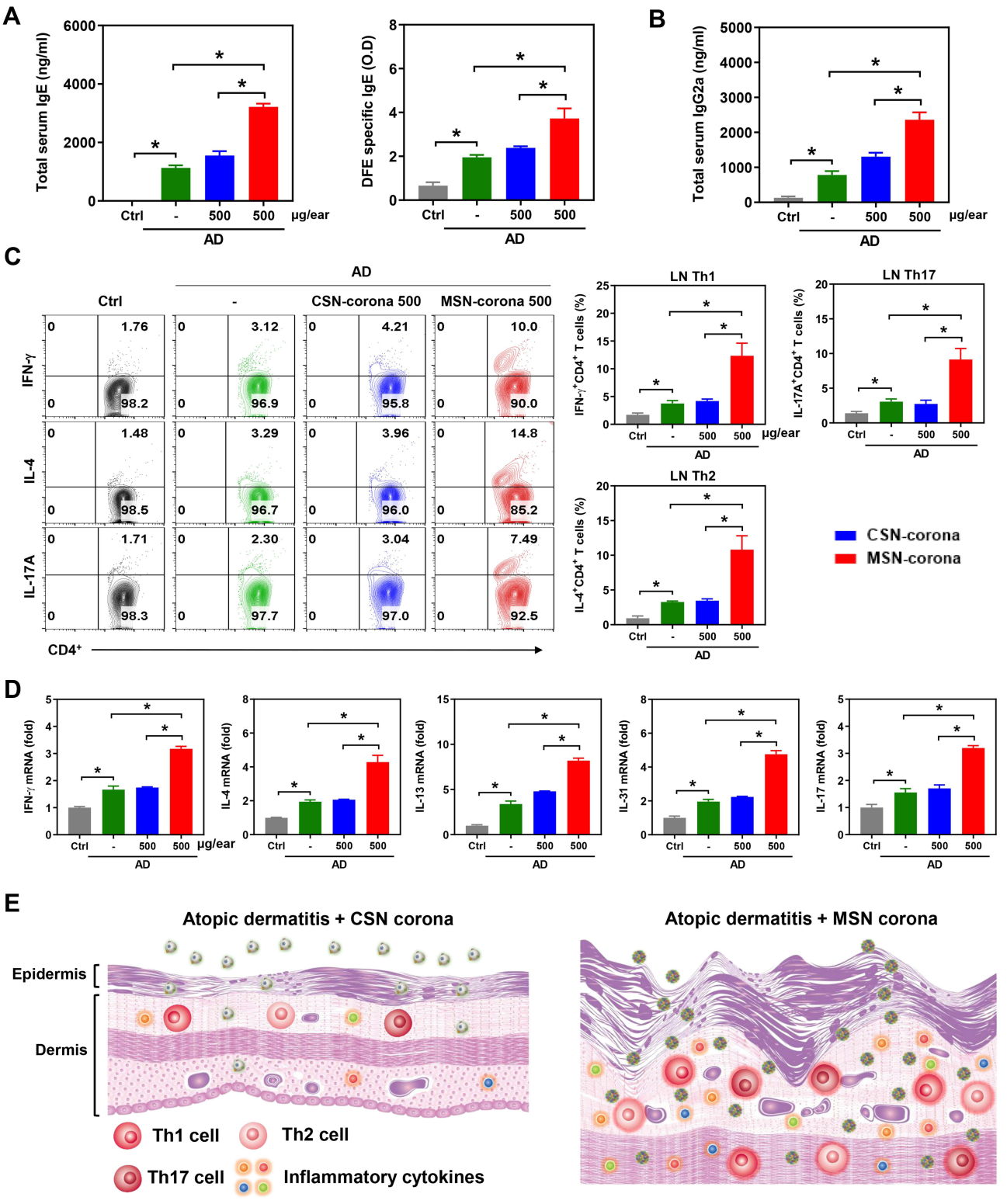

Figure 8 Higher T cell immune responses to MSN in AD skin inflammation. Serum total IgE, DFE-specific IgE (**A**), and serum total IgG2a (**B**) levels were measured using ELISA. Blood samples of various groups, the vehicle (Ctrl), DFE plus the vehicle, and DFE plus nanoparticles, were collected by an orbital puncture on day 21. (**C**) $CD4^+$ T cells in LNs of mice treated with CSN-Corona or MSN-Corona on day 21 after AD induction were analyzed by intracellular cytokine staining for FACS analysis. Numbers in quadrants indicate the percentages of cells expressing $CD4^+$ IFN-γ, IL-4, or IL-17A. Statistical analysis of IFN-γ-, IL-4-, or IL-17-expressing $CD4^+$ T cells in the LNs. (**D**) Expression of cytokines in the ears of CSN-Corona- or MSN-Corona-treated AD mice. To determine the cytokine levels in mice, the ears were excised on day 21. Gene expression was analyzed using qPCR. The gene expression levels were normalized to the β-actin level, and the values of fold-changes are presented. (**E**) Schematic illustration of T cell-mediated immune reactions from AD skin tissues upon MSN and CSN treatment. The data are presented as the mean ± SD of five determinations. *$P < 0.05$.

Abbreviations: AD, DFE-induced atopic dermatitis; CSN, colloidal silica nanoparticles; MSN, mesoporous silica nanoparticles.

Changes in the biological environment may have crucial effects on the formation of protein corona.[48] For example, the type and concentration of serum, incubation time, temperature, and the physiological condition of plasma that is affected by diseases or treatment can affect protein adsorption onto the nanoparticle surface.[36,49] A recent study has shown that protein-corona formation is dependent on the surface area rather than nanoparticle size.[49] Protein coronas on nanoparticle surfaces can control the function of nanoparticles by modulating the amount absorbed by cells.[50] In this study, we have shown that the size, surface charge, and chemical composition of CSN and MSN were not significantly different. The only difference between the two materials is the surface area, which arises from the porosity of the MSN. We observed that MSN formed greater protein coronas on the surface of nanoparticles and showed greater absorption into keratinocytes through caveolae- and clathrin-mediated endocytosis than CSN. Silica nanoparticles (70 nm) have been shown to induce high levels of ROS production and DNA damage in HaCaT cells through cell absorption.[4] These results indicate that the amount of MSN (160 nm) absorbed into keratinocytes was increased because of the protein-corona formation, rather than the direct absorption of MSN into the keratinocytes.

Cytokines are important signaling molecules that regulate cellular activities, inflammation, and hemostasis in vitro and in vivo.[39] They activate the immune system and cause tissue inflammation, opening tight junctions. For example, proinflammatory cytokines such as TNF-α, IL-1β, and IL-6 modulate tight junctions.[39] A decrease in claudin-1 level, an important component of tight junctions, leads to increased intracellular permeability, resulting in unlimited intracellular transport of large proteins and molecules.[39] In our study, MSN was transported into cells because the non-specific protein corona adsorbed onto the MSN surface increased the expression of proinflammatory cytokines and chemokines, which recruit dermal inflammatory cells in AD. Consequently, claudin-1, which regulates junction molecules in keratinocytes, was downregulated. In particular, the functional association between claudin-1 and MSN with non-specific protein coronas was demonstrated by inactivation of the protein corona using BSA adsorption on the surface of CSN or MSN. Overall, other than small lipophilic molecules, other molecules are unlikely to penetrate the skin because of the presence of physical skin barrier factors such as claudin-1. However, we observed that keratinocytes absorbed MSN surrounded by a protein corona, which promoted inflammatory responses and damaged the skin barrier, highlighting the potential association of these MSN with AD.

Previous studies have evaluated the skin penetration of nanoparticles after local application using in vitro and in vivo systems.[9,51,52] However, there is controversy regarding whether nanoparticles cross the skin barrier in vivo and affect the immune system. TiO_2 and ZnO nanoparticles are essential components of sunscreens. Several studies have demonstrated that nanoparticles with sizes of 10–50 nm cannot penetrate healthy skin or tape-stripped skin.[53,54] Additionally, we previously evaluated changes in skin inflammation after application of CSN and MSN (~100 nm diameter) to the skin for 3 consecutive days.[26] We observed that changes in ear thickness were small. These results indicate that the tight junctions of the skin and stratum corneum act as effective barriers against the penetration of nanomaterials into healthy skin. Furthermore, neither CSN nor MSN caused any changes associated with AD, even after repeated local application to the skin of healthy mice.

Simultaneous exposure to nanoparticles and allergens contributes to the aggravation of AD.[54] Several studies have demonstrated the toxic effects of silica nanoparticles on AD after topical skin painting.[55] In our study, topical skin painting using a mixture of MSN and DFE allergens aggravated the clinical symptoms of AD mice. Additionally, these mice exhibited significant increases in inflammatory cellular activity, serum IgE and IgG2 production, Th1/Th2/Th17 immune responses in skin tissues, and draining of the lymph nodes compared to mice treated with DFE alone. We further speculated that increased levels of DFE and proteins in the blood and biological fluids produced during AD attach to the porous surface of MSN to form a protein corona. These MSNs are subsequently absorbed by the epidermal cells in the mouse skin; they move to the draining lymph node to activate inflammatory T-cells and to the skin tissues to induce inflammation. Additionally, the increased levels of T cell-mediated inflammatory cytokines by MSN in skin tissues further weaken claudin-1 and enable unlimited penetration of external allergens into the cell, accelerating the aggravation of AD.

Conclusion

Most nanoparticles have difficulty in penetrating healthy skin; thus, there is a small risk of destroying immune homeostasis after topical application.[54] We showed that MSN increases protein corona formation and protein adsorption in the plasma compared to CSN. Although MSN-corona did not cause inflammation of the healthy skin in the animal model, it caused

inflammation to AD-affected skin tissues. This suggests that MSN-corona destroyed the tight junction protein, claudin-1, in the keratinocytes of the epidermis of the weakened skin in AD, thereby infiltrating into the dermis and aggravating the inflammation. Patients with allergic diseases such as AD and those with skin damage experience increased symptoms such as fever, itchiness, rash, and eczema after exposure to sunlight. Therefore, sunscreens and moisturizers must be used to minimize exposure to sunlight. Our findings suggest that the application of skincare products or sunscreen containing MSN can lead to the formation of protein corona in the skin and biological fluids of patients with AD; the MSN can penetrate deeply into the skin and disrupt immune homeostasis, resulting in aggravated AD symptoms. Therefore, it is necessary to develop technologies that can control the adsorption of proteins onto the porous surface of MSN[56] in skincare products. Such studies may provide further information required to improve the safety and efficacy of MSNs.

Acknowledgments

This work was supported by National Research Foundation of Korea grants funded by the Korean government (2022R1C1C2013133, 2022M3A9H1014123, 2019R1A2B5B01069444, and 2021R1C1C1006089).

Author Contributions

All authors made a significant contribution to the work reported, whether that is in the conception, study design, execution, acquisition of data, analysis, and interpretation, or in all these areas; took part in drafting, revising, or critically reviewing the article; gave final approval of the version to be published; have agreed on the journal to which the article has been submitted; and agree to be accountable for all aspects of the work.

Disclosure

The authors report no conflicts of interest in this work.

References

1. Chan WCW, Chhowalla M, Farokhzad O, et al. The 15th anniversary of the US national nanotechnology initiative. *ACS Nano*. 2018;12(11):10567–10569. doi:10.1021/acsnano.8b08676
2. Park JY, Kwon S, Kim SH, Kang YJ, Khang D. Triamcinolone-gold nanoparticles repolarize synoviocytes and macrophages in an inflamed synovium. *ACS Appl Mater Interfaces*. 2020;12(35):38936–38949. doi:10.1021/acsami.0c09842
3. Park JY, Hyun JS, Jee JG, Park SJ, Khang D. Structural deformation of MTX induced by nanodrug conjugation dictate intracellular drug transport and drug efficacy. *Int J Nanomedicine*. 2021;16:4943–4957. doi:10.2147/IJN.S317231
4. Nabeshi H, Yoshikawa T, Matsuyama K, et al. Amorphous nanosilica induce endocytosis-dependent ROS generation and DNA damage in human keratinocytes. *Part Fibre Toxicol*. 2011;8:1. doi:10.1186/1743-8977-8-1
5. Athinarayanan J, Periasamy VS, Alsaif MA, Al-Warthan AA, Alshatwi AA. Presence of nanosilica (E551) in commercial food products: TNF-mediated oxidative stress and altered cell cycle progression in human lung fibroblast cells. *Cell Biol Toxicol*. 2014;30(2):89–100. doi:10.1007/s10565-014-9271-8
6. Yu T, Greish K, McGill LD, Ray A, Ghandehari H. Influence of geometry, porosity, and surface characteristics of silica nanoparticles on acute toxicity: their vasculature effect and tolerance threshold. *ACS Nano*. 2012;6(3):2289–2301. doi:10.1021/nn2043803
7. Shahbazi MA, Hamidi M, Makila EM, et al. The mechanisms of surface chemistry effects of mesoporous silicon nanoparticles on immunotoxicity and biocompatibility. *Biomaterials*. 2013;34(31):7776–7789. doi:10.1016/j.biomaterials.2013.06.052
8. Chenthamara D, Subramaniam S, Ramakrishnan SG, et al. Therapeutic efficacy of nanoparticles and routes of administration. *Biomater Res*. 2019;23:20. doi:10.1186/s40824-019-0166-x
9. Rancan F, Gao Q, Graf C, et al. Skin penetration and cellular uptake of amorphous silica nanoparticles with variable size, surface functionalization, and colloidal stability. *ACS Nano*. 2012;6(8):6829–6842. doi:10.1021/nn301622h
10. Smith DM, Simon JK, Baker Jr JR Jr. Applications of nanotechnology for immunology. *Nat Rev Immunol*. 2013;13(8):592–605. doi:10.1038/nri3488
11. Ke PC, Lin S, Parak WJ, Davis TP, Caruso F. A Decade of the Protein Corona. *ACS Nano*. 2017;11(12):11773–11776. doi:10.1021/acsnano.7b08008
12. Jo DH, Kim JH, Son JG, et al. Nanoparticle-protein complexes mimicking corona formation in ocular environment. *Biomaterials*. 2016;109:23–31. doi:10.1016/j.biomaterials.2016.09.008
13. Giulimondi F, Digiacomo L, Pozzi D, et al. Author correction: interplay of protein corona and immune cells controls blood residency of liposomes. *Nat Commun*. 2020;11(1):1697. doi:10.1038/s41467-020-15500-9
14. Park JY, Park SJ, Park JY, et al. Unfolded protein corona surrounding nanotubes influence the innate and adaptive immune system. *Adv Sci*. 2021;8(8):2004979. doi:10.1002/advs.202004979
15. Lee YK, Choi EJ, Webster TJ, Kim SH, Khang D. Effect of the protein Corona on nanoparticles for modulating cytotoxicity and immunotoxicity. *Int J Nanomedicine*. 2015;10:97–113. doi:10.2147/IJN.S72998
16. Weidinger S, Beck LA, Bieber T, Kabashima K, Irvine AD. Atopic dermatitis. *Nat Rev Dis Primers*. 2018;4(1):1. doi:10.1038/s41572-018-0001-z

17. Masuoka M, Shiraishi H, Ohta S, et al. Periostin promotes chronic allergic inflammation in response to Th2 cytokines. *J Clin Invest*. 2012;122(7):2590–2600. doi:10.1172/JCI58978
18. Biedermann T, Skabytska Y, Kaesler S, Volz T. Regulation of T cell immunity in atopic dermatitis by microbes: the Yin and Yang of cutaneous inflammation. *Front Immunol*. 2015;6:353. doi:10.3389/fimmu.2015.00353
19. Brandner JM, Zorn-Kruppa M, Yoshida T, Moll I, Beck LA, De Benedetto A. Epidermal tight junctions in health and disease. *Tissue Barriers*. 2015;3(1–2):e974451. doi:10.4161/21688370.2014.974451
20. Bergmann S, von Buenau B, Vidal YSS, et al. Claudin-1 decrease impacts epidermal barrier function in atopic dermatitis lesions dose-dependently. *Sci Rep*. 2020;10(1):2024. doi:10.1038/s41598-020-58718-9
21. Piquero-Casals J, Carrascosa JM, Morgado-Carrasco D, et al. The role of photoprotection in optimizing the treatment of atopic dermatitis. *Dermatol Ther*. 2021;11(2):315–325. doi:10.1007/s13555-021-00495-y
22. Wang SQ, Tooley IR. Photoprotection in the era of nanotechnology. *Semin Cutan Med Surg*. 2011;30(4):210–213. doi:10.1016/j.sder.2011.07.006
23. Krpetic Z, Anguissola S, Garry D, Kelly PM, Dawson KA. Nanomaterials: impact on cells and cell organelles. *Adv Exp Med Biol*. 2014;811:135–156. doi:10.1007/978-94-017-8739-0_8
24. Larese Filon F, Mauro M, Adami G, Bovenzi M, Crosera M. Nanoparticles skin absorption: new aspects for a safety profile evaluation. *Regul Toxicol Pharmacol*. 2015;72(2):310–322. doi:10.1016/j.yrtph.2015.05.005
25. Kim BE, Leung DYM. Significance of skin barrier dysfunction in atopic dermatitis. *Allergy Asthma Immunol Res*. 2018;10(3):207–215. doi:10.4168/aair.2018.10.3.207
26. Lee S, Yun HS, Kim SH. The comparative effects of mesoporous silica nanoparticles and colloidal silica on inflammation and apoptosis. *Biomaterials*. 2011;32(35):9434–9443. doi:10.1016/j.biomaterials.2011.08.042
27. Leng L, Xiong Q, Yang L, et al. An overview on engineering the surface area and porosity of biochar. *Sci Total Environ*. 2021;763:144204. doi:10.1016/j.scitotenv.2020.144204
28. Kankala RK, Wang SB, Chen AZ. Nanoarchitecting hierarchical mesoporous siliceous frameworks: a new way forward. *iScience*. 2020;23(11):101687. doi:10.1016/j.isci.2020.101687
29. Lee S, Kim MS, Lee D, et al. The comparative immunotoxicity of mesoporous silica nanoparticles and colloidal silica nanoparticles in mice. *Int J Nanomedicine*. 2013;8:147–158. doi:10.2147/IJN.S39534
30. Jang YH, Choi JK, Jin M, et al. House dust mite increases pro-Th2 cytokines IL-25 and IL-33 via the activation of TLR1/6 signaling. *J Invest Dermatol*. 2017;137(11):2354–2361. doi:10.1016/j.jid.2017.03.042
31. Kim MJ, Je IG, Song J, et al. SG-SP1 suppresses mast cell-mediated allergic inflammation via inhibition of FcepsilonRI signaling. *Front Immunol*. 2020;11:50. doi:10.3389/fimmu.2020.00050
32. Zhu M, Nie G, Meng H, Xia T, Nel A, Zhao Y. Physicochemical properties determine nanomaterial cellular uptake, transport, and fate. *Acc Chem Res*. 2013;46(3):622–631. doi:10.1021/ar300031y
33. Liu Y, Workalemahu B, Jiang X. The effects of physicochemical properties of nanomaterials on their cellular uptake in vitro and in vivo. *Small*. 2017;13(43):1701815. doi:10.1002/smll.201701815
34. Lawrence ENR, Chao JI. Role of albumin on the cellular uptake and selective autophagy of nanodiamonds. *FASEB J*. 2017;31. doi:10.1096/fasebj.31.1_supplement.lb132
35. Yan Y, Gause KT, Kamphuis MM, et al. Differential roles of the protein corona in the cellular uptake of nanoporous polymer particles by monocyte and macrophage cell lines. *ACS Nano*. 2013;7(12):10960–10970. doi:10.1021/nn404481f
36. Corbo C, Molinaro R, Parodi A, Toledano Furman NE, Salvatore F, Tasciotti E. The impact of nanoparticle protein corona on cytotoxicity, immunotoxicity and target drug delivery. *Nanomedicine*. 2016;11(1):81–100. doi:10.2217/nnm.15.188
37. Basler K, Bergmann S, Heisig M, Naegel A, Zorn-Kruppa M, Brandner JM. The role of tight junctions in skin barrier function and dermal absorption. *J Control Release*. 2016;242:105–118. doi:10.1016/j.jconrel.2016.08.007
38. Capaldo CT, Farkas AE, Hilgarth RS, et al. Proinflammatory cytokine-induced tight junction remodeling through dynamic self-assembly of claudins. *Mol Biol Cell*. 2014;25(18):2710–2719. doi:10.1091/mbc.E14-02-0773
39. Han X, Zhang E, Shi Y, Song B, Du H, Cao Z. Biomaterial-tight junction interaction and potential impacts. *J Mater Chem B*. 2019;7(41):6310–6320. doi:10.1039/c9tb01081e
40. Leung DYM, Boguniewicz M, Howell MD, Nomura I, Hamid OA. New insights into atopic dermatitis. *J Clin Invest*. 2004;113(5):651–657. doi:10.1172/JCI21060
41. Dillon SR, Sprecher C, Hammond A, et al. Interleukin 31, a cytokine produced by activated T cells, induces dermatitis in mice. *Nat Immunol*. 2004;5(7):752–760. doi:10.1038/ni1084
42. Poulsen LK, Hummelshoj L. Triggers of IgE class switching and allergy development. *Ann Med*. 2007;39(6):440–456. doi:10.1080/07853890701449354
43. Novak N, Simon D. Atopic dermatitis - from new pathophysiologic insights to individualized therapy. *Allergy*. 2011;66(7):830–839. doi:10.1111/j.1398-9995.2011.02571.x
44. Wolk K, Kunz S, Witte E, Friedrich M, Asadullah K, Sabat R. Sabat R. IL-22 increases the innate immunity of tissues. *Immunity*. 2004;21(2):241–254. doi:10.1016/j.immuni.2004.07.007
45. Liu L, Guo D, Liang Q, et al. The efficacy of sublingual immunotherapy with Dermatophagoides farinae vaccine in a murine atopic dermatitis model. *Clin Exp Allergy*. 2015;45(4):815–822. doi:10.1111/cea.12417
46. Werfel T, Allam JP, Biedermann T, et al. Cellular and molecular immunologic mechanisms in patients with atopic dermatitis. *J Allergy Clin Immunol*. 2016;138(2):336–349. doi:10.1016/j.jaci.2016.06.010
47. Knochelmann HM, Dwyer CJ, Bailey SR, et al. When worlds collide: th17 and Treg cells in cancer and autoimmunity. *Cell Mol Immunol*. 2018;15(5):458–469. doi:10.1038/s41423-018-0004-4
48. Park SJ. Protein-nanoparticle interaction: corona formation and conformational changes in proteins on nanoparticles. *Int J Nanomedicine*. 2020;15:5783–5802. doi:10.2147/IJN.S254808
49. Lee SY, Son JG, Moon JH, Joh S, Lee TG. Comparative study on formation of protein coronas under three different serum origins. *Biointerphases*. 2020;15(6):061002. doi:10.1116/6.0000396
50. Rampado R, Crotti S, Caliceti P, Pucciarelli S, Agostini M. Recent advances in understanding the protein corona of nanoparticles and in the formulation of "stealthy" nanomaterials. *Front Bioeng Biotechnol*. 2020;8:166. doi:10.3389/fbioe.2020.00166

51. Hirai T, Yoshikawa T, Nabeshi H, et al. Amorphous silica nanoparticles size-dependently aggravate atopic dermatitis-like skin lesions following an intradermal injection. *Part Fibre Toxicol*. 2012;9:3. doi:10.1186/1743-8977-9-3
52. Nafisi S, Schafer-Korting M, Maibach HI. Perspectives on percutaneous penetration: silica nanoparticles. *Nanotoxicology*. 2015;9(5):643–657. doi:10.3109/17435390.2014.958115
53. Lin LL, Grice JE, Butler MK, et al. Time-correlated single photon counting for simultaneous monitoring of zinc oxide nanoparticles and NAD(P)H in intact and barrier-disrupted volunteer skin. *Pharm Res*. 2011;28(11):2920–2930. doi:10.1007/s11095-011-0515-5
54. Yoshioka Y, Kuroda E, Hirai T, Tsutsumi Y, Ishii KJ. Allergic responses induced by the immunomodulatory effects of nanomaterials upon skin exposure. *Front Immunol*. 2017;8:169. doi:10.3389/fimmu.2017.00169
55. Hirai T, Yoshioka Y, Takahashi H, et al. Cutaneous exposure to agglomerates of silica nanoparticles and allergen results in IgE-biased immune response and increased sensitivity to anaphylaxis in mice. *Part Fibre Toxicol*. 2015;12:16. doi:10.1186/s12989-015-0095-3
56. Kankala RK, Han YH, Na J, et al. Nanoarchitectured structure and surface biofunctionality of mesoporous silica nanoparticles. *Adv Mater*. 2020;32 (23):e1907035. doi:10.1002/adma.201907035